

The effect of intact talin and talin tail fragment on actin filament dynamics and structure depends on pH and ionic strength

Wolfgang H. Goldmann¹, Daniel Hess² and Gerhard Isenberg²

¹Departments of Pathology and Surgery, Children's Hospital, Harvard Medical School, Boston, USA; ²Department of Biophysics, Technical University of Munich, Germany

We employed quasi-elastic light scattering and electron microscopy to investigate the influence of intact talin and talin tail fragment on actin filament dynamics and network structure. Using these methods, we confirm previous reports that intact talin induces cross-linking as well as filament shortening on actin networks. We now show that the effect of intact talin as well as talin tail fragment on actin networks is controlled by pH and ionic strength. At pH 7.5, actin filament dynamics in the presence of intact talin and talin tail fragment are characterized by a rapid decay of the dynamic structure factor and by a square root power law for the stretched exponential decay which is in contrast with the theory for pure actin solutions. At pH 6 and low ionic strength, intact talin cross-links actin filaments more tightly than talin tail fragment. Talin head fragment showed no effect on actin networks, indicating that the actin binding sites reside probably exclusively within the tail domain.

Keywords: talin; focal adhesion complex; actin filament cross-linking; tension.

Focal adhesion complexes (FAC) are crucial points for the regulation of cytoskeletal filament assembly and mechanical linkage in cells. Proteins found in FAC at the intracellular face of the plasma membrane include talin, vinculin, paxillin, and α -actinin, and the order in which these proteins interact with integrin, actin, or each other is still under investigation [1].

Talin is a major protein component of FAC, binds to integrin, vinculin, and actin [2–4] and inserts directly into lipid bilayers [5]. It has a mass of 270 kDa (as deduced from the cDNA sequence [6]) and can be proteolytically cleaved into two regions: a 47-kDa head and 190-kDa tail domain. The head is responsible for membrane attachment [7] and displays considerable homology with other membrane attachment proteins of the cytoskeleton such as band 4.1 or the ERM family (ezrin-radixin-moesin) [8]. The tail domain has a high α -helical content and contains the vinculin and actin binding sites [9] which is made of 50–60 irregularly arranged copies of 35 amino acid repeats [8]. Two functions of intact talin have been reported from measurements with actin: the control of actin filament length and the cross-linking of actin polymers [10,11]. Other studies have also indicated that the binding of F-actin to talin, which significantly increases actin filament stiffness [12], is a two-step-process [13].

In spite of the extensive knowledge of the properties of talin and its distribution, very little is known of its precise mode of interaction with the various junctional and cytoskeletal components in living cells. Only a few investigations so far have given

some indication: e.g. Goldmann *et al.* [14] and Xu *et al.* [15] used a mouse embryonic F9 cell line deficient in vinculin [F9Vin (–/–)] and transfected these cells with vinculin that express vinculin deficient in the talin and α -actinin binding site on vinculin. These cells showed a marked change in cell locomotion and their mechanical and viscoelastic properties compared to the F9 wild-type. Niewöhner *et al.* [16] used a *Dictyostelium* cell line which lacks talin and showed that cell adhesion and motility were impaired, and Priddle *et al.* [17] recently reported that undifferentiated talin (–/–) embryonic stem cells were unable to spread and form focal adhesion-like structures. These findings indicate how important the recruitment of FAC proteins, including talin and vinculin, and the physical linkage of integrins to the cytoskeleton is for dynamic processes [18]. In the present study, we investigated the dynamic properties of semiflexible actin filaments when bound to intact talin and talin tail fragment using quasi-elastic light scattering (QELS) and electron microscopy.

MATERIALS AND METHODS

Proteins and reagents

Actin was prepared according to the method of Pardee and Spudich [19], from acetone powder obtained from rabbit back muscle, with an additional gel filtration step as described by MacLean-Fletcher and Pollard [20]. Biological activity of the purified actin was tested by falling ball viscometry, and its concentration was determined spectrophotometrically using an absorbance coefficient $A_{290\text{ nm}}^{1\%}$ of $26\,460\text{ M}^{-1}\cdot\text{cm}^{-1}$. Fractionated G-actin beyond the elution peak (at $\approx 1\text{ mg}\cdot\text{mL}^{-1}$) was stored on ice in G-buffer (2 mM Tris/HCl, pH 8.0; 0.5 mM ATP, 0.2 mM CaCl_2 , 0.2 mM dithiothreitol and 0.05 vol% NaN_3) and used within 10 days. Polymerization of actin in the presence/absence of intact talin and talin fragments was performed at 4 °C in 2 mM imidazole, 0.2 mM ATP, 0.2 mM CaCl_2 , 0.2 mM dithiothreitol, 2 mM MgCl_2 , and 0.05 vol% NaN_3 at various KCl concentrations and pH.

Correspondence to W. H. Goldmann, Departments of Pathology and Surgery, Children's Hospital, Harvard Medical School, Enders 10, 320 Longwood Ave., Boston MA 02115, USA. Tel: + 1 617 355 6254.

Fax: + 1 617 355 7043, E-mail: GOLDMANN_W@a1.tch.harvard.edu.

URL: [HTTP://www.web1.tch.harvard.edu/research/](http://www.web1.tch.harvard.edu/research/)

Abbreviations: QELS, quasi-elastic light scattering; IT, 270-kDa intact talin; TTF, 190-kDa talin tail fragment; THF, 47-kDa talin head fragment; FAC, focal adhesion complex.

(Received 14 September 1998, revised 3 December 1998, accepted 7 December 1998)

Talin preparation from outdated platelets was performed according to the method of Collier and Wang [21], with an additional gel filtration step [22]. Thrombin cleavage of intact talin (IT) into 190-kDa tail (TTF) and 47-kDa head (THF) fragments was carried out as described below. Protein purity was greater than 99% as judged by SDS/PAGE. The determination of protein concentration was performed by BioRad assay according to the manufacturer's protocol.

Tris and EDTA were from Sigma (Deisenhofen, Germany), dithiothreitol was from Roth (Karlsruhe, Germany), ATP was from Serva (Heidelberg, Germany), thrombin was from Boehringer-Mannheim (Mannheim, Germany), and all other reagents were from Fluka (Deisenhofen, Germany).

Preparation of talin fragments

Talin aliquots ($0.66 \text{ mg}\cdot\text{mL}^{-1}$) were dialyzed against 50 mM Tris/HCl; pH 8.0. Enzymatic cleavage was performed by adding $2 \text{ U}\cdot\text{mg}^{-1}$ thrombin for 2 h. The fragments were then separated on a Mono Q FPLC column (Pharmacia), equilibrated in 50 mM Tris/HCl; pH 8.0. The 47-kDa THF fragment appeared in the flow-through, whereas the 190-kDa TTF fragment was eluted by a linear NaCl gradient [13].

Quasi-elastic light scattering

The basic setup of the light scattering apparatus described by Pieckenbrock and Sackmann [23] was used throughout. Thus, improvements were made by replacing the correlator (ALV 5000 from ALV, Langen, Germany). This device has 1024 parallel channels and contains a more sensitive photomultiplier. The photomultiplier uses a 'pseudo cross-correlation' method with a much improved signal-to-noise ratio. The correlator contains the ALV 5000/E and ALV5000 'fast' card which allow precise measurements and calculation of the intensity correlation function over a logarithmic time scale ($0.5 \mu\text{s}$ –10 s) using 328 channels. An Innova coherent 70-4 argon-ion laser of 200 mW was used for the 488 nm spectral line. Prior to QELS measurements, all solutions were filtered (pore size $0.22 \mu\text{m}$) and stored overnight at 4°C to achieve equilibrium of polymerization.

Electron microscopy

Electron microscopy was performed on a Zeiss CEM 902 as described previously [24]. Briefly, samples are adsorbed on glow-discharged carbon-coated Formvar films on copper grids and negatively stained with uranyl acetate (0.5% w/v, pH 4.0).

Theoretical basis of quasi-elastic light scattering

It is assumed that networks of polymerized actin consist of single filaments at a diameter a , with a contour length L up to $30 \mu\text{m}$, and a persistence length l_p of $\approx 17 \mu\text{m}$, and that the wavevector $q = 2\pi/\lambda$ corresponds to the length smaller than the average meshsize x_m to fulfill the condition $a \ll \lambda \ll l_p$ and $\lambda < x_m$ [25]. In our analysis, we used the mathematical description in terms of the 'Rouse-like' Langevin equation for transverse bending undulations: $\zeta_{\perp}(d/dt)r_s^{\perp}(t) = -k(\partial/\partial s^4)r_s^{\perp}(t) + f_s^t$ where ζ_{\perp} is an appropriate friction coefficient (per length), k is the bending modulus and f_s^t is the stochastic force. For the friction coefficient, we assume $\zeta_{\perp} = (4\pi\eta/\ln(\Lambda/a))$ for $\lambda \approx x_m$ (Λ is the hydrodynamic screening length) and $\zeta_{\perp} = [(4\pi\eta)/(5/6) - \ln(qa)]$ for $\lambda \ll x_m$ and q is the wavevector. For the hydrodynamic screening length Λ , we assume $\Lambda \approx x_m \sim c_A^{-1/2}$

where c_A is the concentration of actin (see [26] for further reading).

Detailed calculations by Kroy and Frey [27] show that in the intermediate time regime, the decay of the dynamic structure factor $g(k,t)$ is a good approximation of a stretched exponential with an exponent of $3/4$: $g(k,t) = g(k,0) \exp\{-[\Gamma(0.25)/3\pi](\gamma_k t)^{3/4}\}$. The decay rate, $\gamma_k = (k_B T/\zeta_{\perp})k^{8/3}l_p^{-1/3}$ depends on the filament stiffness through the persistence length l_p , and the mesh size (or actin concentration c_A) enters through Λ into the appropriate friction coefficient ζ_{\perp} . By using, $\gamma_k = (k_B T/\zeta_{\perp})k^{8/3}l_p^{-1/3}$ it is possible to describe the decay of the dynamic structure factor in QELS experiments for actin networks.

RESULTS

Actin filament dynamics in the presence of intact talin at pH 7.5

The decay of the dynamic structure factor of actin filament networks in the presence of IT was followed over the entire

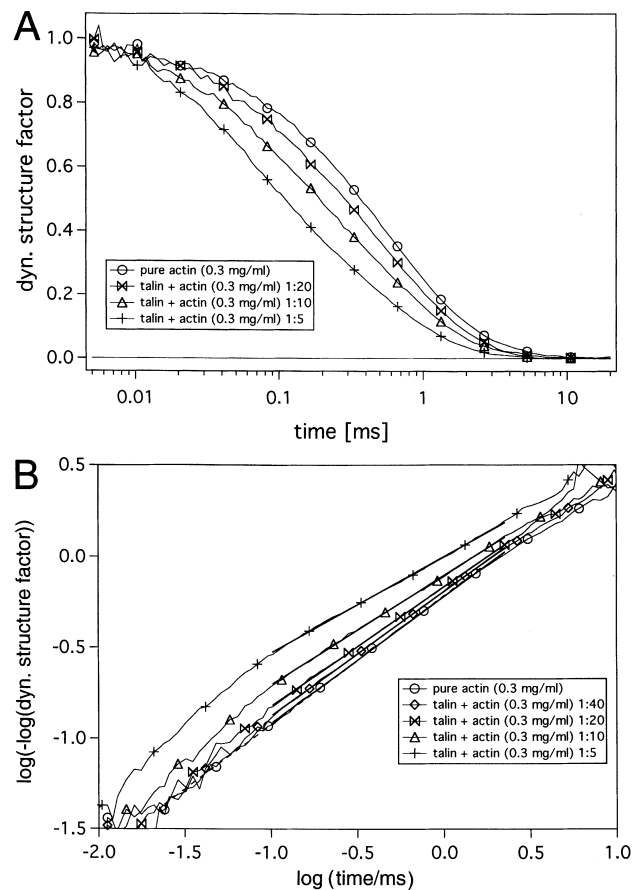


Fig. 1. Influence of IT on actin filament dynamics. (A) Plot of the decay curves for various IT concentrations with time at a scattering angle of 86° . The decay of the dynamic structure factor of actin networks in the presence of IT was measured with time at pH 8.0. At an F-actin concentration of $0.3 \text{ mg}\cdot\text{mL}^{-1}$, the molar ratios of IT were 1 : 5 (+), 1 : 10 (Δ), 1 : 20 (\times) and 1 : 40 (\diamond). Pure actin was used as control (O). Note that the trace for a molar ratio of actin/IT 1 : 40 is not shown for clarity. (B) Evaluation of the exponent of the stretched exponential in the intermediate time regime by double-logarithmic plots. The exponents: pure actin = 0.70; IT/actin at 1 : 40 = 0.67; IT/actin at 1 : 20 = 0.65; for IT/actin at 1 : 10 = 0.59; and for IT/actin at 1 : 5 = 0.53.

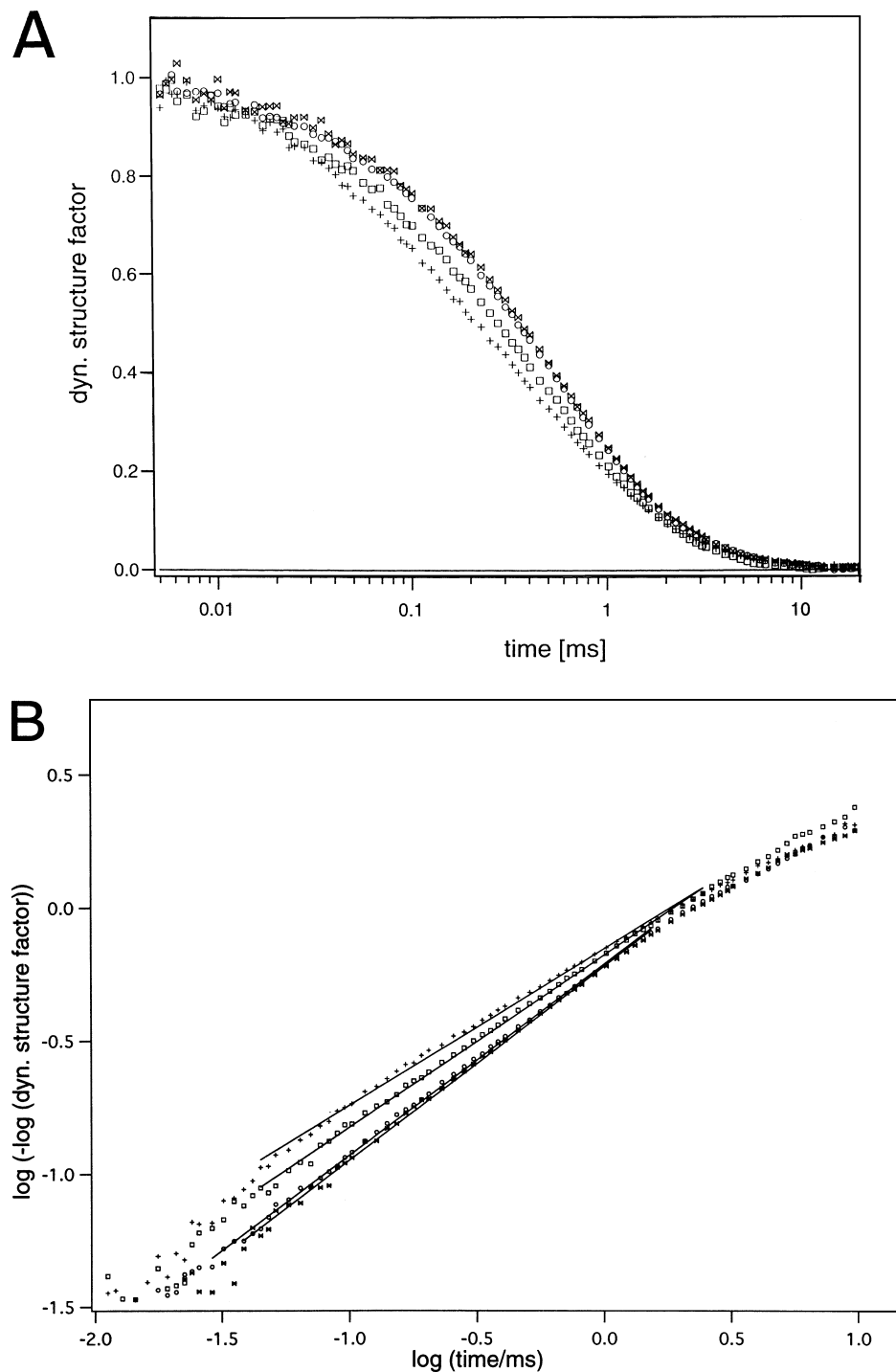


Fig. 2. Influence of THF and TTF on actin filament dynamics. (A) The decay at a scattering angle of 86° of the dynamic structure factor of actin networks in the presence of TTF and THF under the conditions described in Fig. 1: pure actin (\circ), actin molar ratio of 1 : 10 IT (+), TTF (\square) and THF (\times). (B) The corresponding double-logarithmic plots indicating an exponent (= slope) of 0.72 for pure actin; 0.73 for THF; 0.63 for TTF; and 0.56 for IT.

correlation time at 10 different scattering angles (from 30° to 130°) at IT/actin molar ratios from 1 : 40 to 1 : 5. We observed, with increasing IT concentration, a significant shift of the dynamic structure factor decay curve to shorter correlation times (Fig. 1A at 86° angle). This behavior is indicative of a change in exponent of the stretched exponentials shown in the double logarithmic Kohlrausch plot (Fig. 1B). In the intermediate time regime characterized by the linear slope, the exponents of the single stretched exponential decreased with increasing protein concentration. At the highest IT/actin molar ratio (1 : 5), the exponent approached a numerical value of $1/2$ compared to $3/4$ for pure actin [27]. The time regime depicted by the linear slope

changed from 0.3 to 3 ms for actin in the presence of IT (Fig. 1B, top trace) and from 0.03 to 0.3 ms for pure actin (Fig. 1B, bottom trace). The region between the initial decay and semiflexible regime is also extended to longer correlation times when actin polymerized in the presence of IT (Fig. 1B). All of these observations are indicative of higher actin filament mobility due to filament shortening. This assumption was confirmed by electron microscopy studies (compare Fig. 5A and Fig. 5B). Both graphs show homogeneous network distribution; however, actin filaments polymerized in the presence of IT (Fig. 5B) appeared less dense and somewhat disrupted. The average number of crossing filaments per area was much lower

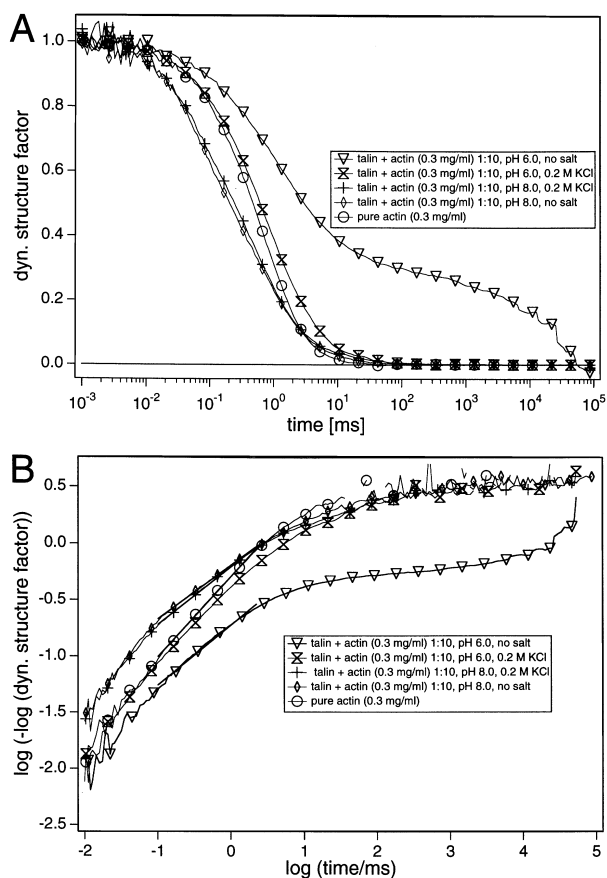


Fig. 3. Effect of pH and ionic strength on IT-actin interaction. (A) Plot of decay curves at a scattering angle of 86° . The actin polymerization was performed under the conditions described in Fig. 1. Pure actin solutions were polymerized at pH 6.0, without added KCl (\circ). Actin in the presence of IT at a molar ratio of 1 : 10 was polymerized at pH 6.0 in the presence (0.2 M KCl, \diamond), absence of KCl (\triangle), and at pH 8.0 in the presence 0.2 M KCl, (+) and absence of KCl (\square). (B) The corresponding double-logarithmic plot shows an exponent (= slope) of 0.75 for pure actin; 0.72 for IT/actin at pH 6.0 in presence of 0.2 M KCl; 0.62 for IT/actin at pH 6.0 and no added KCl; and 0.58 for IT/actin at pH 8.0 in the presence/absence of 0.2 M KCl.

than for pure actin which was probably due to the filament shortening effect of talin.

Actin filament dynamics in the presence of talin tail fragment at pH 7.5

Several studies have indicated that the functional actin binding site(s) reside within TTF [9,28]. To provide further evidence, we examined the effect of IT, THF, and TTF on actin filament dynamics by QELS (Fig. 2A and B). At a talin/actin molar ratio of 1 : 10, only IT and TTF but not THF, exerted a shift to shorter correlation times. This is clearly demonstrated in the Kohlrausch plot (Fig. 2B). In the intermediate time regime, a decrease in the slope of IT and TTF was observed, but not for THF. The effect of TTF on actin filament dynamics, however, was less pronounced than that of IT at the same molar ratio. This is demonstrated by the slopes in the intermediate time regime: 0.56 for IT-actin and 0.63 for TTF-actin networks, respectively; and by the larger shift to shorter correlation times for IT (Fig. 2B).

Actin filament cross-linking induced by intact talin at pH 6

The internal dynamics of actin filaments in the presence of IT were altered dramatically upon changes in pH of the polymerizing solution from 8.0 to 6.0 at low ionic strength (Figs 3A, 3B and 5C). At low pH and low ionic strength, the decay of the dynamic structure factor shifted to longer correlation times with a correlation plateau ranging from 10 ms to 1 s (Fig. 3A). This behavior can be explained in terms of 'phase separation' where a homogenous network (here, actin polymerizing in the presence of IT at high pH) changes to a microgel state with a locally condensed network (here, actin polymerizing at lower pH and low ionic strength). The electron microscopy work demonstrated these coexisting phases, exhibiting tightly packed, globular domains within loosely arranged actin filament networks (Fig. 5C).

Complete inhibition of talin's actin cross-linking ability was observed at pH 6, when 200 mM KCl was added to the polymerization buffer. The correlation decay was shifted marginally to longer correlation times (Fig. 3A and B), and no visible differences were observed compared to pure actin networks

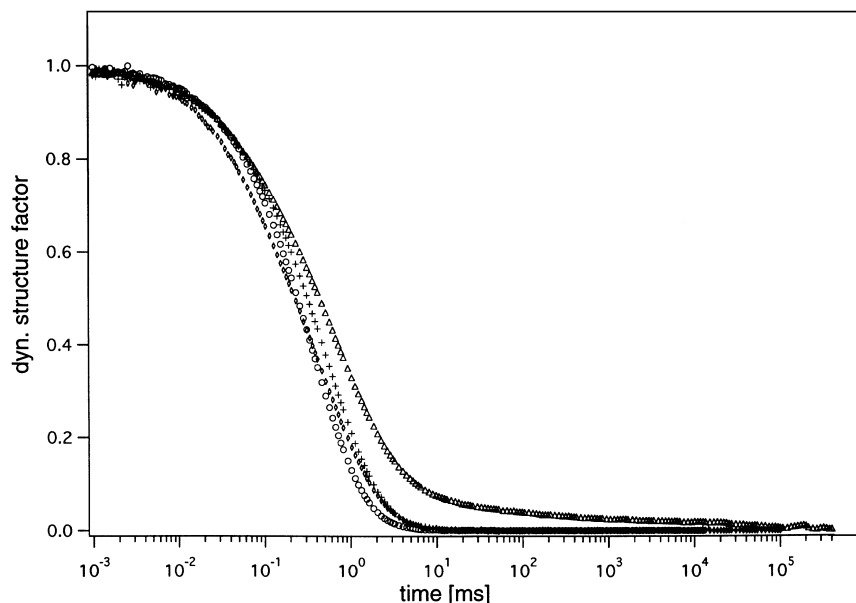


Fig. 4. Cross-linking of actin filaments by TTF.

Cross-linking of actin at a concentration of $0.2 \text{ mg}\cdot\text{mL}^{-1}$ by TTF at a molar ratio of 1 : 10 and pH 6.0 measured at a scattering angle of 90° . Pure actin solution was polymerized at pH 6.0, in the presence of 0.2 M KCl, (+) and without added KCl (\circ). TTF/actin at 1 : 10 molar ratio was polymerized in the presence of 0.2 M KCl, (\diamond) and absence of KCl (\triangle).

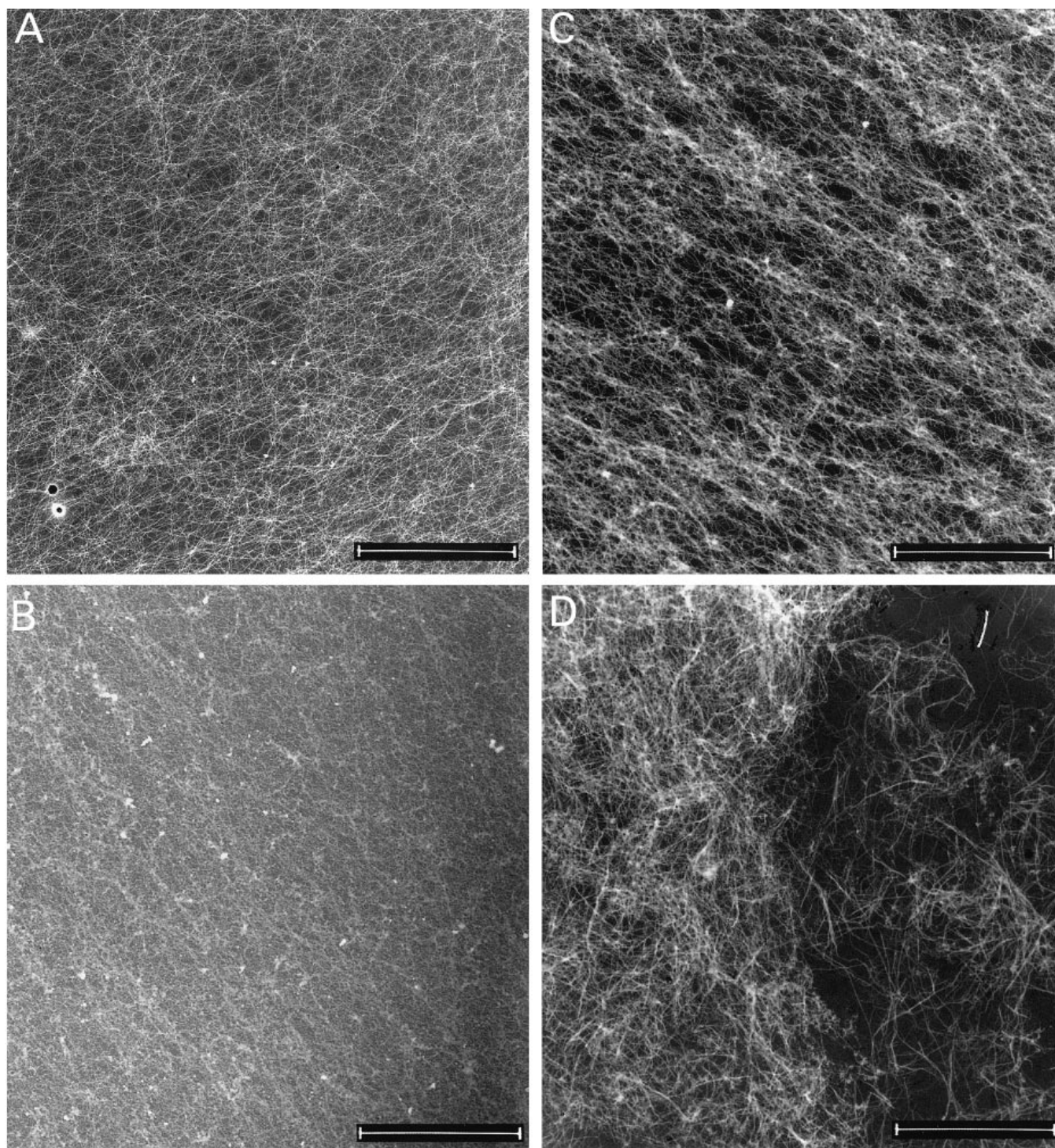


Fig. 5. Electron micrographs of actin solutions in the presence/absence of talin. Electron micrographs of solutions used in QELS measurements. (A) Pure actin solution ($0.3 \text{ mg}\cdot\text{mL}^{-1}$) polymerized at pH 8.0 in the presence of 0.2 M KCl (cf. Fig. 1). (B) Actin polymerized in the presence of IT at a molar ratio of 1 : 5 at pH 8.0 and in the presence of 0.2 M KCl (cf. Fig. 1). (C) Actin polymerized in the presence of IT at a molar ratio 1 : 10 and pH 6.0 with no added KCl (cf. Fig. 2). (D) Actin polymerized in the presence of TTF at pH 6.0 with no added KCl (cf. Fig. 4). Bar = $5 \mu\text{m}$.

(data not shown). However, adding 200 mM KCl at pH 8.0 had no effect on talin's actin filament shortening ability.

Actin network dynamics in the presence of talin tail fragment

Actin was polymerized in the presence of TTF at a molar ratio of 10 : 1 and at pH 6.0 in the presence/absence of 200 mM KCl (Fig. 4). QELS measurements showed similar results for the

effects of TTF and IT on actin filament dynamics. At pH 6.0, TTF shifted the autocorrelation function to longer decay times, an effect which could be reversed by increasing the ionic strength to 200 mM KCl. The effect of TTF on actin was less notable compared to IT: a smaller shift in exponent, and the complete absence of a plateau region indicated reduced cross-linking. Fig. 5D demonstrates the condensing effect that TTF has on actin networks at pH 6.0 and low ionic strength,

Table 1. Summary of exponents determined by stretched exponential fit analysis in Figs 1B, 2B and 3B.

Fragment (molar ratio)	Exponents from stretched exponential fits			Pure actin (control)
	IT	TTF	THF	
From Fig. 1B				0.70
IT/actin, 1 : 40	0.67			
IT/actin, 1 : 20	0.65			
IT/actin, 1 : 10	0.59			
IT/actin, 1 : 5	0.53			
From Fig. 2B				0.72
IT/actin, 1 : 10	0.56			
TTF/actin, 1 : 10		0.63		
THF/actin, 1 : 10			0.73	
From Fig. 3B				0.75
IT/actin, 1 : 10, pH6.0				
+ 0.2 M KCl	0.72			
- 0.2 M KCl	0.62			
IT/actin, 1 : 10, pH8.0				
+/- 0.2 M KCl	0.58			

exhibiting areas of higher electron density and larger spacing between actin filaments compared to IT (Fig. 5C).

DISCUSSION

In the present study, we employed a much improved QELS detection method to investigate the pH and ionic strength dependence of IT and TTF on actin filament dynamics. Using an extended theory for the dynamic light scattering analysis, which was initially derived for pure actin solutions, we established that QELS can be applied as a reliable tool for detecting filament shortening and changes in actin gels. We confirm observations from previous kinetic studies that the biphasic binding process of IT and TTF to F-actin under conditions described here is due to F-actin cross-linking [13].

Using IT and TTF in actin polymerization assays, actin filaments are shorter and show a narrower distribution of length compared with pure actin. This phenomenon can be explained by talin's ability to nucleate actin [22]; however, when comparing the influence of, e.g. gelsolin (unpublished data) and talin on actin filament dynamics considerable differences are apparent. Although both proteins reduce the overall actin filament length, filament shortening induced by gelsolin shows a different behavior. At low gelsolin concentration the 'general term' for the decay of the dynamic structure factor still applies, however, at increasing gelsolin concentration the scale separation condition is no longer valid i.e. the filament movement is no longer dominated by bending undulations but also by the rotation of short filaments. At very high gelsolin concentrations, the system can be described as 'diffusion of short rigid rods' with an exponent of 1 for the stretched exponential. Contrary to these observations we found, in this study, a decrease of the exponent of the stretched exponential from 3/4 (pure actin) to 1/2 at the highest actin/IT molar ratio. A possible explanation for this behavior comes from work by Caspi *et al.* [29] who investigated the strain induction in microtubules by applying optical tweezers. These researchers showed that the exponent of the mean square displacement function, which is related to the autocorrelation decay in QELS, of actin filaments shifted from 3/4 (unstrained, subdiffusive regime) to 1/2 (strained regime). Intriguingly, actin filaments cross-linked by α -actinin also showed a slope in the intermediate time regime close to 1/2 (0.54 at a actin/ α -actinin molar ratio of 10 : 1 at 9 °C and pH 7;

unpublished observation). Findings in this study suggest that the decrease of the exponent of the stretched exponential from 3/4 to 1/2 is the result of tension induced by talin binding and subsequent cross-linking of actin filaments. Caspi *et al.* [29] pointed out that filament tension scales with k^2 , whereas bending elasticity scales with k^4 . Therefore, even tension induced, e.g. by weak cross-linker or distortion of filaments by actin binding proteins will result in a square root power law decay of the stretched exponential. Summarizing the effects on actin, we believe that: (a) between pH 7.5 and 8.0 IT and TTF shorten actin filaments and induce filament tension by distortion or weak cross-linking; (b) between pH 7.0 and 6.0 and low ionic strength IT and TTF cross-link actin filaments (Table 1). These effects point to a salt- and pH-dependent oligomerization and/or exposition of the binding sites on the talin molecule. The factors controlling the association state of this molecule are currently the focus of our research.

The distribution of talin's functional actin binding sites on TTF was also of interest. As shown in Figs 2 and 4, only TTF influences actin filament dynamics and no effect was observed by THF. This suggests that the highly conserved THF contains no functional actin binding site, although it might have some influence on the actin binding site(s) of TTF. Support for this view comes from our observations that the influence of TTF on actin filament dynamics in the absence of THF is somewhat reduced compared with the effects of IT.

When looking at cross-linking at acidic pH and low ionic strength in cells deficient of talin or talin binding sites on vinculin local changes in pI should be considered [30]. In studies using mouse embryonic F9 cells that are deficient of the talin and α -actinin binding sites, Xu *et al.* [15] showed that the tail fragment of vinculin probably binds actin and the lipid membrane in a way that prevents the vinculin tail from making the changes necessary for cell attachment, spreading, and locomotion. These authors argue that intact vinculin is necessary to act as a molecular bridge for cellular dynamic functions. Similarly, Niewöhner *et al.* [16] suggested that the loss of talin in *Dictyostelium* cells fails to provide the molecular integrity and full level control of the focal adhesion complex, and Sydor *et al.* [31] found talin to be critical for filopodial motility in neuronal growth cones.

In recent studies of F9 cell lines, in which we measured the effect of intracellular pH at different ionic strength on cell dynamics by using an analysis system based on (2',7'-bis-(2-carboxyethyl)-5-(and-6)-carboxyfluorescein) pH-sensitive indicator dye and 495/440 nm ratio imaging, we observed changes in spreading and a reduced rate of motility. Taken together with the observations of the present study, these first results are encouraging, although further *in vivo* studies are needed to elucidate talin's and vinculin's function as molecular linking proteins between the actin cytoskeleton and the lipid membrane [32].

ACKNOWLEDGEMENTS

We acknowledge Drs Klaus Kroy (E.S.P.C.I., Physique Thermique, Paris), Erich Sackmann and Roman Goetter (TU, Muenchen), Fred McIntosh (University of Michigan) and Donald E. Ingber (Harvard Medical School, Boston) for helpful discussions. We thank Ms. I. Sprenger for electron microscopy, Dr. S. Kaufmann for the preparation of talin and talin fragments, Ms. M. Hohenadl for helping with experiments, and Ms. J. Feldmann for careful reading of this manuscript. This work was supported by grants from the Deutsche Forschungsgemeinschaft (SFB 266/C-5, Is 25/7-2). W.H. Goldmann is a recipient of a collaborative research grant from the North Atlantic Treaty Organization.

REFERENCES

- Janmey, P.A. (1998) The cytoskeleton and cell signaling: component localization and mechanical coupling. *Physiol. Rev.* **78**, 763–781.
- Horwitz, A., Duggan, K., Buck, C., Beckerle, M. & Burridge, K. (1986) Interaction of plasma membrane fibronectin receptor with talin – a transmembrane linkage. *Nature* **320**, 531–533.
- Burridge, K. & Mangeat, P. (1984) An interaction between vinculin and talin. *Nature* **308**, 744–746.
- Goldmann, W.H. & Isenberg, G. (1991) Kinetic determination of talin-actin binding. *Biochem. Biophys. Res. Commun.* **178**, 718–723.
- Goldmann, W.H., Niggli, V., Kaufmann, S. & Isenberg, G. (1992) Probing actin and liposome interaction of talin and talin–vinculin complexes: a kinetic, thermodynamic and lipid labeling study. *Biochemistry* **31**, 7665–7671.
- Rees, D.J.G., Ades, S.E., Singer, S.J. & Hynes, O. (1990) Sequence and domain structure of talin. *Nature* **347**, 685–689.
- Niggli, V., Kaufmann, S., Goldmann, W.H., Weber, T. & Isenberg, G. (1994) Identification of functional domains in the cytoskeletal protein talin. *Eur. J. Biochem.* **224**, 951–957.
- McLachlan, A.D., Stewart, M., Hynes, R.O. & Rees, D.J.G. (1994) Analysis of repeated motifs in the talin rod. *J. Mol. Biol.* **235**, 1278–1290.
- Hemmings, L., Rees, D.J., Ohanian, V., Bolton, S.J., Gilmore, A.P., Patel, B., Priddle, H., Trevithick, J.E., Hynes, R.O. & Critchley, D.R. (1996) Talin contains three actin-binding sites each of which is adjacent to a vinculin-binding site. *J. Cell Science* **109**, 2715–2726.
- Muguruma, M., Matsumura, S. & Fukazawa, T. (1992) Augmentation of alpha-actinin-induced gelation of actin by talin. *J. Biol. Chem.* **267**, 5621–5624.
- Zhang, J., Robson, R.M., Schmidt, J.M. & Stromer, M.H. (1996) Talin can cross-link actin filaments into both networks and bundles. *Biochem. Biophys. Res. Commun.* **218**, 530–537.
- Ruddies, R., Goldmann, W.H., Isenberg, G. & Sackmann, E. (1993) The viscoelasticity of entangled actin networks: the influence of defects and modulation by talin and vinculin. *Eur. Biophys. J.* **22**, 309–321.
- Goldmann, W.H., Guttenberg, Z., Kaufmann, S., Hess, D., Ezzell, R.M. & Isenberg, G. (1997) Examining F-actin interaction with intact talin and talin head and tail fragment using static and dynamic light scattering. *Eur. J. Biochem.* **250**, 447–450, and (1998) **254**, 207.
- Goldmann, W.H., Galneder, R., Ludwig, M., Xu, W., Adamson, E.D., Wang, N. & Ezzell, R.M. (1998) Differences in elasticity of vinculin-deficient F9 cells measured by magnetometry and atomic force microscopy. *Exp. Cell Res.* **239**, 235–242.
- Xu, W., Coll, J.L. & Adamson, E.D. (1998) Rescue of mutant phenotype by reexpression of full-length vinculin in null F9 cells: effects on cell locomotion by domain deleted vinculin. *J. Cell Sci.* **111**, 1535–1544.
- Niewöhner, J., Weber, I., Maniak, M., Müller-Taubenberger, A. & Gerisch, G. (1997) Talin-null cells of *Dictyostelium* are strongly defective in adhesion to particle and substrate surfaces and slightly impaired in cytokinesis. *J. Cell Biol.* **138**, 349–361.
- Priddle, H., Hemmings, L., Monkley, S., Woods, A., Patel, B., Sutton, D., Dunn, G.A., Zicha, D. & Critchley, D.R. (1998) Disruption of the talin gene compromises focal adhesion assembly in undifferentiated but not differentiated embryonic stem cells. *J. Cell Biol.* **142**, 1121–1133.
- Ingber, D.E. (1997) Tensegrity: The architectural basis of cellular mechanotransduction. *Ann. Rev. Physiol.* **59**, 575–599.
- Pardee, J.D. & Spudich, J.A. (1982) Purification of muscle actin. *Meth. Enzymol.* **85** (B), 164–181.
- MacLean-Fletcher, S.D. & Pollard, T.D. (1980) Identification of a factor in conventional muscle actin preparations which inhibits actin filament self-association. *Biochem. Biophys. Res. Commun.* **96**, 18–27.
- Collier, N. & Wang, K. (1982) Purification and properties of human platelets p235. *J. Biol. Chem.* **257**, 6937–6943.
- Kaufmann, S., Pieckenbrock, T.H., Goldmann, W.H., Bärmann, M. & Isenberg, G. (1991) Talin binds to actin and promotes filament nucleation. *FEBS Lett.* **284**, 187–191.
- Pieckenbrock, T.H. & Sackmann, E. (1992) Quasi-elastic light scattering study of thermal excitations of F-actin solutions and of growth kinetics of actin filaments. *Biopolymers* **32**, 1471–1489.
- Goldmann, W.H., Tempel, M., Sprenger, I., Isenberg, G. & Ezzell, R.M. (1997) Viscoelasticity of actin-gelsolin networks in the presence of filamin. *Eur. J. Biochem.* **246**, 373–379.
- Ott, A., Magnasco, M., Simon, A. & Libchaber, A. (1993) Measurement of the persistence length of polymerized actin using fluorescence microscopy. *Phys. Rev. Lett.* **E48**, R1642–R1645.
- Götter, R., Kroy, K., Frey, E., Bärmann, M. & Sackmann, E. (1996) Dynamic light scattering from semidilute actin solutions: a study of hydrodynamic screening, filament bending stiffness, and the effect of tropomyosin/troponin binding. *Macromolecules* **29**, 30–36.
- Kroy, K. & Frey, E. (1997) Dynamic scattering from solutions of semiflexible polymers. *Phys. Rev. Lett.* **E55**, 3092–3101.
- McCann, R.O. & Craig, S.W. (1997) The I/LWEQ module: a conserved sequence that signifies F-actin binding in functionally diverse proteins from yeast to mammals. *Proc Natl Acad. Sci. USA* **94**, 5679–5684.
- Caspi, A., Elbaum, M., Granek, R., Lachish, A. & Zbaida, D. (1998) Semiflexible polymer network: a view from inside. *Phys. Rev. Lett.* **80**, 1106–1109.
- Tempel, M., Goldmann, W.H., Isenberg, G. & Sackmann, E. (1995) Interaction of the 47-kDa talin fragment and the 32-kDa vinculin fragment with acidic phospholipids: a computer analysis. *Biophys. J.* **69**, 228–241.
- Sydor, A.M., Su, A.L., Wang, F.S., Xu, A. & Jay, D.G. (1996) *J. Cell Biol.* **134**, 1197–1207.
- Goldmann, W.H., Ezzell, R.M., Adamson, E.D., Niggli, V. & Isenberg, G. (1996) Vinculin, talin and focal adhesions. *J. Muscle Res. Cell Motil.* **17**, 1–5.